Electrochimica Acta 124 (2014) 52–60

Contents lists available at ScienceDirect

Electrochimica Acta

journal homepage: www.elsevier.com/locate/electacta

Influence of Unsupported Concrete Media in Corrosion Assessment for Steel Reinforcing Concrete by Electrochemical Impedance Spectroscopy

A.S. Castela[a,b,*], B. Sena da Fonseca[a,c], R.G. Duarte[a,b], R. Neves[b], M.F. Montemor[a]

[a] ICEMS, DEQ, Instituto Superior Técnico, University of Lisbon, 1049-001, Lisboa, Portugal
[b] Instituto Politécnico de Setubal, ESTBarreiro, 2389-001 Barreiro, Portugal
[c] CICEGe, Faculdade de Ciências e Tecnologia, Universidade Nova de Lisboa, 2829-516 Caparica

ARTICLE INFO

Article history:
Received 13 April 2013
Received in revised form
19 November 2013
Accepted 27 November 2013
Available online 11 December 2013

Keywords:
Concrete
EIS
Unsuported media
Permeability

ABSTRACT

This work aims at studying the response of unsupported concrete media by Electrochemical Impedance Spectroscopy (EIS) and its influence in the results obtained for steel corrosion in reinforced concrete samples. Measurements carried out in full immersed samples correspond to a typical electrolyte media, presenting essentially a resistive behavior. Thus, rebar corrosion, which appears commonly at intermediate frequency region, can be assessed and easily interpreted.

For samples in partial dry conditions the spectra show several time-constants distributed across the entire frequency range. In the high frequency region, the time constant is ascribed to dielectric properties of the system. At low frequencies the time constant corresponds to the ionic depletion, while the time constant at intermediate frequencies result from charge separation inside the material bulk, typically of unsupported media. Interpretation of the results obtained by EIS for concrete reinforced steel in partial dry conditions cannot be fully interpreted without considering the dielectric behavior of the system.

1. Introduction

One of the most important problems in concrete durability is related to fluids uptake. Water, fog and air from the environment are the most important carriers of harmful elements. The characteristics of the pore system play a decisive role in engineering properties of concrete [1]. Moreover, concrete mechanical properties such as strength, durability and permeability are function of the material porosity [2]. High permeability causes a faster penetration of solutions, resulting in rapid concrete deterioration [3,4]. From this point of view, the interaction between harmful ions (like chlorides and sulfates) and the steel reinforcement could lead to severe corrosion threatening the whole structure.

By this reason, in the last decades, several authors have studied the reinforcement corrosion activity in concrete by Electrochemical Impedance Spectroscopy, EIS [5–10]. One of the most common environmental conditions that promote corrosion involves dry or partial dry-conditions especially, dry-wet cycles, which play a crucial role in what concerns corrosion activity. In such conditions concrete becomes an unsupported media and the obtained results are an expression of steel corrosion and concrete impedance response. Theoretical studies presented by Macdonald *et al.* [11,12] interpreted the phenomenon of EIS in unsupported media by taking into consideration that the complexity of the response must be related with charge separation inside the film bulk.

For measurements carried out in partial dry conditions, particularly associated with dry-wet cycles, the results are affected by ions, water and gases transport. This can occur by three mechanisms: permeability, diffusion and absorption [13]. These mechanisms are governed by the pore structure, which is characterized by the porosity, connectivity between pores and pore size [14], which is the main factor influencing the porosity is water-cement ratio (w/c) [15]. However, other factors, like cement type, can also affect the porosity [16]. Nevertheless, the tests to assess the permeability coefficients are long and relatively complicated [17]. EIS technique is a very suitable technique to determine concrete properties, such as permeability. Several authors have already used this non-destructive technique to reveal the microstructure of concrete [18,19].

It is well known that Fickian diffusion process is an analogue problem to Fourier heat conduction and 2nd Fick law describes the diffusion process in a transient-state. For a short diffusion times,

* Corresponding author.
E-mail addresses: antonio.castela@estbarreiro.ips.pt, antoniocastela@netcabo.pt (A.S. Castela).

0013-4686/$ – see front matter © 2013 Elsevier Ltd. All rights reserved.
http://dx.doi.org/10.1016/j.electacta.2013.11.157

that is, for the beginning of diffusion in a membrane with parallel surfaces, the profile of any specie diffusing inside the membrane is given by the following equation [20,21]:

$$\frac{c_0 - c}{c_0 - c_s} = erf\left(\frac{x}{2\sqrt{Dt}}\right) \quad (1)$$

in which D is the diffusion coefficient, t is the time, x is the distance inside the membrane bulk to the surface and c, c_s, and c_0 are the specie concentration at distance x for time t, saturation (s) and dry condition (0), respectively. To derive this equation several other conditions were considered, such as: the thickness of the diffusion layer must be much smaller than the membrane thickness, d, if diffusion occurs only at one surface side, or half the membrane thickness, if the diffusion occurs at both surfaces, and Fourier number is given by $Fo = Dt/d^2 < 0.05$; For the beginning of diffusion, $t = 0$, the concentration is residual, $c = c_0$; The concentration is maximum, $c = c_s$, at membrane surface, $x = 0$, while for $x \rightarrow d$ the concentration is residual, $c = c_0$ [22,23]. This equation was used in concrete samples by several authors [24–26]. In such conditions integration of equation 1 throughout all the membrane dimensions allows to obtain another equation that permits to determine the average diffusion coefficient for the early stages of diffusion [20,27–30]:

$$\frac{\phi_0 - \phi}{\phi_0 - \phi_s} = \frac{4\sqrt{D}}{d\sqrt{\pi}}\sqrt{t} \quad (2)$$

in which ϕ, ϕ_s, and ϕ_0 are the specie uptake for time t, saturation (s) and dry condition (0), respectively. To apply this equation to a membrane (coating, polymer, concrete, etc.) it is necessary to estimate the ϕ, ϕ_s, and ϕ_0 values using several experimental results such as impedance, gravimetric measurements, etc.

This work aims at studying the response of unsupported concrete media by EIS and its influence in the results obtained for reinforcing steel corrosion in concrete samples.

2. Experimental

Six different concrete mixtures were designed with the aim of covering a range of water-cement ratio (w/c) typically encountered in reinforced concrete and considering the type of cements most commonly used. Limestone coarse aggregates and natural silica sand were used. Characteristics of the concrete mixes are summarized in Table 1. The mixing time was about 5 minutes. More details about the concrete mixes and mixing procedures can be found elsewhere [32]. The tests were performed in small cylinders (150 mm diameter and 50 mm tall) sawn from larger ones (150 mm diameter and 300 mm tall). The original specimens were removed from molds at 24 hours and kept in tepid (20 °C) water for 7 days.

The 300 mm tall cylinders were sawn in slices of 50 mm which were coated with a double layer of adhesive aluminum in their molded (curved) surface. In the conditioning period, between the end of curing and permeability testing, which occurred after 28 days, all specimens were kept in a laboratory chamber at 20 °C and 60% RH. The specimens were kept in the conditions of the conditioning period between the end of the permeability tests and EIS tests.

Air permeability was assessed, using a test method developed by Torrent [33], which presents a good correlation with oxygen permeability assessed by Cembureau method [34], the latter of which is recommended by RILEM TC 116-PCD [35] and considered as "reference test" by RILEM TC 189-NEC [36] to characterize gas permeability. Compared to Cembureau, the Torrent method has the advantage of being faster, since gas permeability is assessed in a non-steady state. The principle of the test is to create a certain degree of vacuum in the test chamber using a vacuum pump and then cut the connection between the vacuum pump and the test chamber and measure the rate at which pressure increases in the latter. This makes it possible to calculate air permeability coefficient kT associated with this method [37].

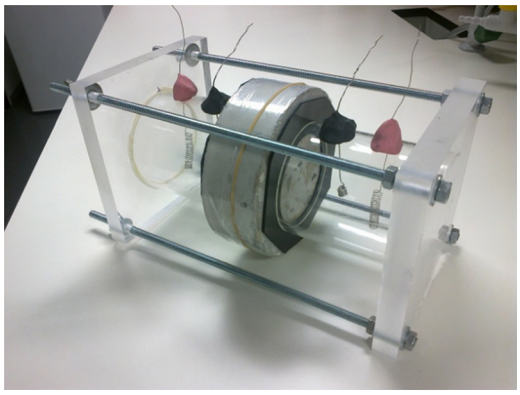

Fig. 1. Picture of a four electrodes arrangement cell used for the saturation tests.

The saturation tests were performed using a 1% sodium chloride (NaCl) solution in the two-compartment cell and using a four-electrode arrangement. The concrete sample was held between the compartments, with two smaller platinum electrodes working as pseudo-reference electrodes and two larger platinum electrodes acting as counter electrodes (fig. 1). To avoid the short-circuiting of the current by the surrounding environment rubber washers were used on both sides between the container and the samples. The transversal area exposed to the electrolyte was 50.12 cm^2, while 176.71 cm^2 was the total transversal area of the samples. The ratio between the total area and the exposed one was 3.5.

For the drying tests, a two electrode arrangement cell was used, in which two plates of stainless steels (316L), with 100 cm^2 each and the ratio between the total area and the exposed one was 1.77, were compressed against the sample flat faces, operating each one simultaneously as counter and reference electrode (fig. 2). For the saturation tests the EIS measurements started about 30 seconds after full-immersion and were carried out until saturation occurs, that is, until low frequency impedance were stabilized, between 14.5 hours and 145 hours depending of samples type. The samples were kept in immersion during at least 1 week to guarantee that full-saturation condition was achieved for all of them. Afterwards, samples were removed from solution and assembled in the two-electrode arrangement cell. The EIS drying tests started about 2 minutes after samples were removed from solution. These tests were performed continuously during 120 hours to 180 hours until the samples dryness imposes difficulties for EIS measurements and spectra stabilization occurred.

The EIS measurements were conducted using a Zanher Zennium Electrochemical Workstation. The frequency range used at the

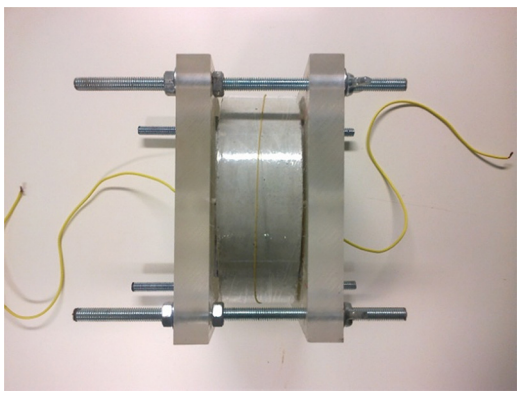

Fig. 2. Photograph of a two electrodes arrangement cell used for the drying tests.

Table 1
concrete samples main characteristics.

Cement [31]	Cement content (kg m^3)	w/c ratio	Strength Class	Plasticizer
CEM I	356	0.39	C 55/67	Polycarboxylic ether
CEM I	340	0.46	C 40/50	Polycarboxylic ether
CEM I	310	0.53	C 35/45	Modified Lignosulfonate
CEM I	280	0.60	C 30/37	Modified Lignosulfonate
CEM II/A	370	0.51	C 30/37	Commercial: Sikament 190
CEM IV/A	310	0.53	C 25/30	Modified Lignosulfonate

beginning of each test (20 minutes) was between 2 kHz and 4 MHz. For longer times, the frequency range used was between 50 mHz and 4 MHz. The applied amplitude was 50 mV (rms). Numerical fitting of the impedance data was made using *ZView*® software. The samples remain in a controlled environment chamber at 25 °C during the saturation and drying tests

3. Results and Discussion

3.1. EIS measurements

Fig. 3 depicts the EIS spectra evolution with time during saturation and drying tests for a representative sample (CEM I; w/c = 0.39). The spectra are strongly dependent on the environmental conditions. Measurements carried out in a 4-electrodes cell (Fig. 3a) during saturation tests showed that concrete behaves as a typical electrolyte media, presenting only a resistive behavior, except at very high frequencies where a dielectric time constant can be observed. At this frequency range, and with such high impedance values, the influence of cables is negligible; however, two explanations can be given for this time constant, one corresponds to the dielectric response of the system the other considers artifacts given by the equipment limits. This result agrees with literature, in which the resistive behavior for mortar samples was identified as being strongly related with the concentration solution inside de pores and the Friedel's salt formation. On the other hand, the dielectric behavior has two contributions one related with the solid phase and the other refers to solution pore structure [38–40]. Nevertheless the rebar corrosion, which appears commonly at intermediate frequency region, can be assessed and easily interpreted since concrete response in this frequency region is influenced only by the media resistance. There are published works made by other authors, which already take that in consideration [6,7, 9 and 19]. As expected, the concrete resistance depends upon the solution content dropping with the increase in the saturation degree with immersion time. The time constant observed at very high frequency becomes less visible for low impedance values, i.e., for higher solution content values.

During drying test (Fig. 3b) the impedance spectra obtained are unexpectedly different, presenting several time-constants distributed across the entire frequency region. Therefore spectra interpretation for concrete reinforced steel obtained in such partial dry conditions is quite challenging. As previously, the time constant appearing at high frequency region can be currently interpreted either considering the dielectric response of the system or artifacts given by the equipment limits. At low frequencies the time constant can easily be understood, since the samples are not immersed, thus the continuous ionic displacement during measurements cannot be replaced and ionic depletion takes place. To explain this, it must be considered that current always flows through the easiest path; in this situation the current in saturated samples results from the ionic flow, however, for the drying test there is no external ions reservoir, thus for very low frequencies the ionic species already migrated and charges with the same signal starts to accumulate and, consequently, charge separation occurs. The impedance increased since charge accumulation becomes progressively difficult as consequence of the ionic depletion. It can be stated that the bulk cannot be considered infinite and for very low frequencies the EIS results are progressively independent of the sample ionic content. Moreover, impedance grows very fast with increasingly predominance of the concrete matrix response, i.e., preponderance of the imaginary part of impedance. It must be stated that this behavior has been reported in other types of systems such as membranes, detached coatings, etc. The time-constant most difficult to interpret is the one appearing at intermediate frequency region. However, these results appear only in drying tests samples and becomes progressively relevant for longer drying times. That is an indicator that concrete low solution content is related with this phenomenon. M. Cabeza et al. [41] already reported that at high frequency region (100 kHz to 40 MHz) hardened Portland cement paste showed two time constants, relating the pore structure of the samples and a contribution of the solution inside the sample. C. Andrade et al. [42] reported that a time constant, relating the hardened Portland cement paste structure, can be detected at frequencies higher than 1 MHz, ascribing the 100 kHz to 1 MHz time constant to interfacial phenomenon.

A detailed observation of the EIS results shows a general trend, in which the main characteristics of the different spectra seem to be a snap-shot of a continuous evolution triggered by the environmental changes. Thus, for full immersion conditions, and near the sample saturation, the spectra are essentially resistive. For the initial drying hours, when the samples still retain in their pores a considerable amount of solution, the spectra show three time constants (fig. 4a). There is one always present in the high frequency region and another one in the low frequency region that is related with depletion processes. The third one, observed in the intermediate frequency range, results from the continuous decreasing of the solution content in concrete bulk, which indicates an evolution of the concrete media from a poor ionic conductor to an insulating material that can be described as an unsupported media. Consequently, the impedance response can be caused by the mobility differences between the cations and anions in the pore solution, i.e., ions charge separation occurs [11,12] that becomes progressively visible in EIS spectra. The best interpretation for these results is given by an equivalent circuit proposed by Macdonald *et al.* [11], which must be modified by introducing a third time constant, to account for the depletion process. That phenomenon could be originated either by low solution content or by solution with low ionic strength. Fig. 5a shows the modified equivalent circuit in which the capacitances must be replaced by constant phase elements (CPEs) to account for depression in the time constants, resulting essentially from the high heterogeneity of the samples, and with the purpose of obtaining a better fitting result. It must be stated that the equivalent circuits presented here are valid for the frequency range tested and the resistance element that can be detected in direct current (DC) tests is not present.

Finally, for longer drying times the spectra shows four time constants (fig. 4b). The fourth one appears in the high frequency range and its interpretation can only be made if charge separation is considered. As stated before, to interpret these results, it should be considered that the drying concrete sample is an unsupported media, in which the solution is constrained in small volumes

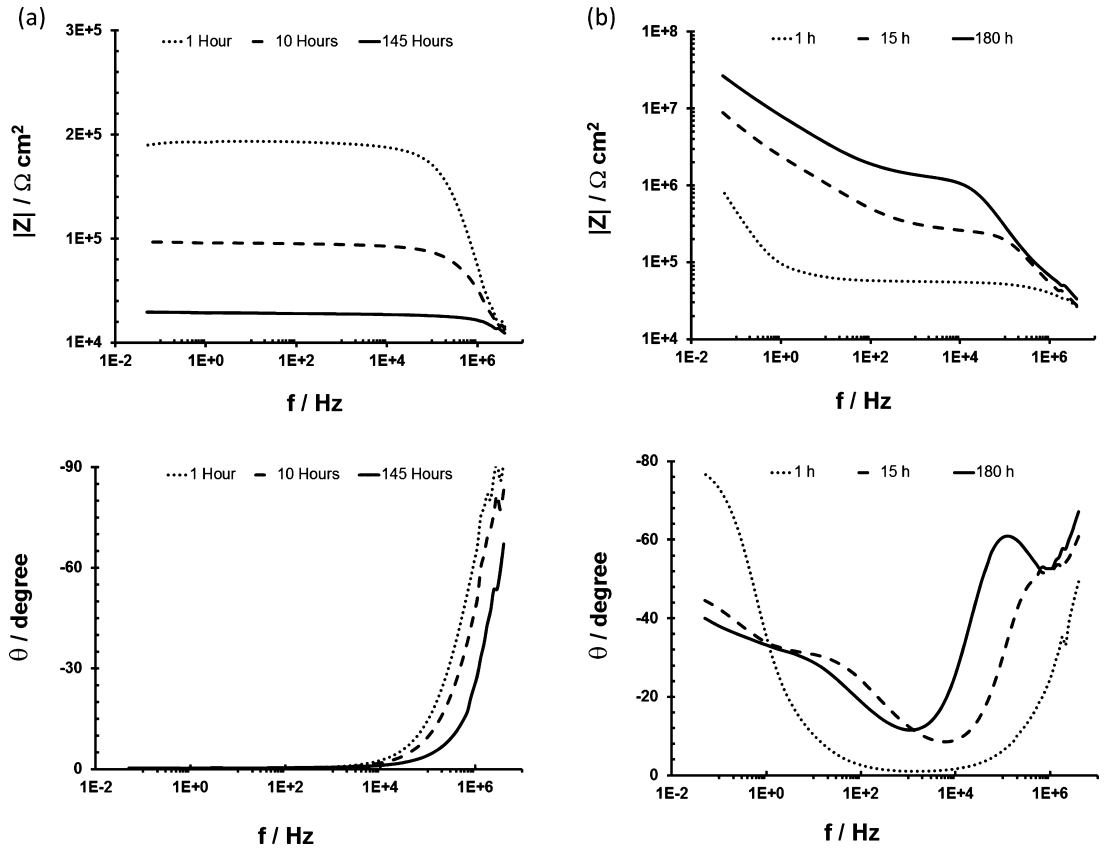

Fig. 3. Bode diagrams showing the evolution of the impedance modulus and phase, angle with time for concrete sample with CEM I and with w/c = 0.39: (a) saturation test, and (b) drying test.

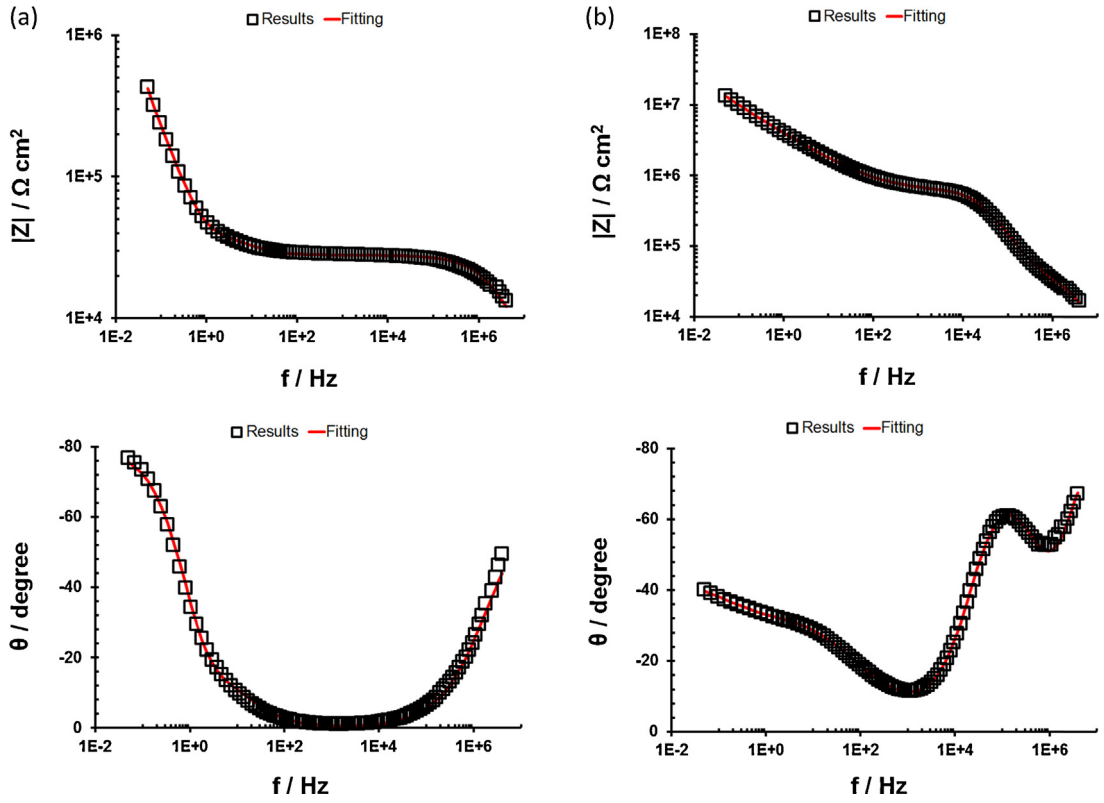

Fig. 4. Fitting results for EIS spectra obtained from concrete samples with CEM I, and with w/c = 0.39, during drying tests, after (a) 1 hour and (b) 180 hours of drying.

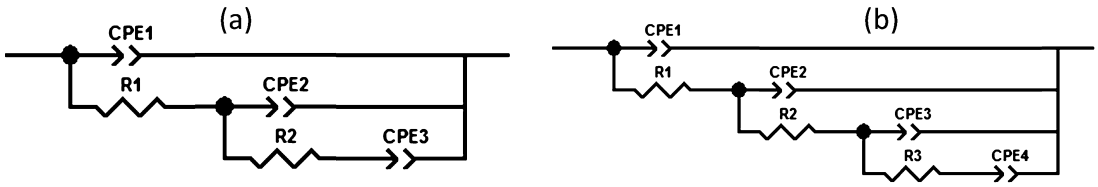

Fig. 5. Equivalent circuits used for fitting the EIS spectra results obtained from, drying tests: (a) short drying time condition and (b) long drying time condition.

(pores) and without an external ions feed. In such situation, as reported by Macdonald et al. [11], a time constant appears because of charge separation. This phenomenon is frequency dependent because if the applied frequency is very high then the change rate of the electric field is so intense that even the time response for the more mobile ions is insufficient to induce any displacement (migration) and no time constant is observed. However, as the frequency decreases, the more mobile ions start to migrate, promoting charge separation; consequently a time constant is detected. Therefore, the frequency at which the time constant appears must be related with the ions mobility and for lesser mobile ions the time constant appears at lower frequencies. This interpretation needs the presence of two types, or classes, of ionic species with very different and independent mobilities, i.e., that do not participate in a common process (ex: reaction). That is the case of concrete samples since the interstitial electrolyte has a very high concentration of mobile ions such as Ca^{2+}, OH^{-}, Na^{+}, Cl^{-}, etc., but there are also much slower mobile ions such as superplasticizers in all samples. Furthermore the superplasticizers are much more voluminous comparatively with the others very mobile smaller ions. Thus, the mobility must be severely affected by the pores dimension and by the adsorption phenomenon; also the solubility of this species have constrains. All these factors should increase the mobility gap between both classes of ions. Consequently, the results can now be understood, assuming that at early drying stages, the time constant developing at intermediate frequency ranges is given by the charge separation of superplasticizers ionic species, while the second time constant, appearing in the high frequency region, for more dried samples, can only be ascribed to the more mobile ions. Another interpretation for these time-constants can be given considering different pore types, namely, pores with different radius classes, however, such explanation cannot describe the appearing of these time constants only for the drying concrete, which becomes more evident with drying time. Moreover, to interpret the presence of two time constants at both high and low frequencies as processes resulting only from different pore classes is unlikely, since the frequency gap is enormous. This explanation is not consistent with the presence of two well-defined time constants.

The EIS results obtained from samples in saturation tests are very simple and the apparent resistance values can be estimated. According to B. Díaz et al. [43], measurements made in immersed ionic material samples, such as cementitious ones, in which only a partial transversal area is exposed, are affected by the conducting occurring at the fringe of the samples, i.e., the transversal part of the samples that is not in contact with the electrolyte can originate current dispersion inside the sample. This phenomenon influences the resistance values of the analysed samples, causing apparent resistivity values lower than the real ones. Therefore any parameter obtained from these results can be defined as an apparent one and, considering the geometry of the samples and cells, the resistivity values determined are half of the real ones. Nevertheless, since the geometry of the samples and cells and the ratios of the total/exposed areas are identical for all the samples, in each type of test, then all the results are affected in identical extent and comparative conclusions can be drawn.

The study of the dried samples results is more complex and here the fitting routines become helpful. The studies presented by B. Díaz et al. [43] were made only in immersed samples, however, the same kind of phenomenon must appear for dried samples, but with less significance, especially for longer drying times. Thus, Table 2 depicts the apparent fitting parameters for EIS results obtained after 100 hours of drying for concrete samples manufactured with CEM I. In these conditions the adequate equivalent circuit is the one appropriated for longer drying times, presenting 4 time constants. At very high frequency the time constant is essentially given by a capacitor, since the depression parameter is unitary. The values of the capacitance are in the range of 2.2 to 2.5 pF cm^{-2} (220 to 250 pF), which is a small capacitance but that values are accordingly with M. Colazo [41]. Considering that the sample thickness is 5 cm and the area of the stainless steel electrodes is 100 cm^2, then for longer drying times the estimated dielectric constant is about 124, which is much higher than the minimum reading limit value ($\varepsilon = 1$). The impedance modulus at 4 MHz, obtained from samples even after 100 hours of drying, are on the range of 10^4 Ω cm^2 (100 Ω), which according with the accuracy map of the device [http://www.zahner.de/pdf/b_zennium.pdf; 15, July, 2013] is a measurement that can be obtained with maximum precision, i.e., 2% error and 3° deviation. It should be emphasized that all the measurement were obtained in a Faraday cage and a preliminary study on this problem was also made, in which several materials was tested such as wood, very high resistance concrete with expanded clay, reference tests with cells without concrete samples containing only electrolytes of different resistivity. Also commercial resistor elements from 90 Ω to 5 GΩ were tested. The aim of these tests was to discard the influence of the equipment in the measurements obtained by the device around the 4 MHz range. The results showed that when measurements are performed outward the device limits, quite different outcomes are obtained with phase

Table 2
Fitted parameters for concrete samples manufactured with CEM I cement and with different w/c ratios, after 100 hours of drying (the units of R_1, R_2 and R_3 are in Ω cm^2 while Y_0 units are S s^n cm^{-2}).

CEM I (w/c)	Drying test (t = 100 h)										
	CPE1		R1	CPE2		R2	CPE3		R3	CPE4	
	Y_0	n		Y_0	n		Y_0	n		Y_0	n
0.39	2.2E-12	1	3.4E+04	3.6E-11	0.90	3.5E+05	1.2E-07	0.52	5.5E+06	8.8E-08	0.53
0.46	2.2E-12	1	2.9E+04	3.5E-11	0.90	4.4E+05	8.0E-08	0.54	7.0E+06	2.4E-08	0.80
0.53	2.3E-12	1	1.9E+04	6.4E-11	0.85	2.4E+05	1.5E-07	0.49	4.0E+06	9.6E-09	0.79
0.60	2.5E-12	1	1.7E+04	9.9E-11	0.83	1.6E+05	2.2E-07	0.47	4.0E+07	7.4E-08	0.76

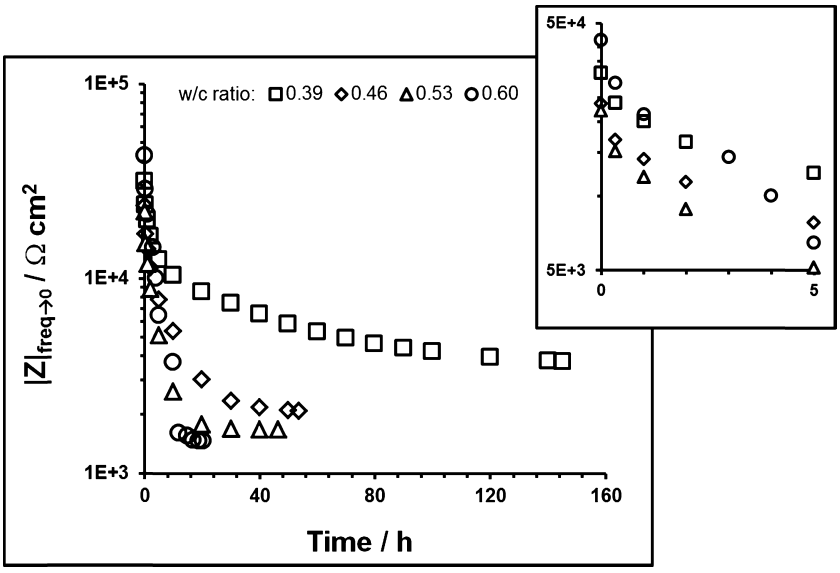

Fig. 6. Evolution of the impedance modulus at the lowest frequency (2 kHz) with, resistive behavior ($\theta = 0^\circ$) with time for concrete samples with CEM I and for different, w/c ratio, obtained during saturation test.

angle lower than -100° at high frequency, however, if device limits are not reached then even at 4 MHz the phase angle is higher than -90°, depending of the tested object. This occurs for resistors with resistance lower than 4.7 kΩ, reference tests and for the concrete samples in which the phase angle never were inferior to -70°. For resistors with resistances similar to the concrete samples, the phase angle imposed is $\theta \rightarrow 0^\circ$ at 4 MHz. Thus, it can be concluded that at very high frequency the time constant corresponds to the dielectric behavior of the system. From this response the contact between the electrode and the sample surface cannot be excluded [42].

Evidently, samples with higher w/c ratio correspond to a more porous medium. Therefore, after saturation these samples must present higher solution content and should retain more solution and humidity, comparatively with the less porous ones, whenever in the same conditions. That was observed in all the estimated apparent resistance parameters, which presented lower resistance values for higher w/c ratios, however, differences are not significant. An inverse trend could be observed for the values of constant phase elements. The fitting parameters obtained for the samples made with 0.5 w/c ratio and with different cement types, after 100 hours of drying, are presented in table 3. The values are coherent between the samples, presenting resistances and CPEs parameters values in the same order of magnitude.

3.2. Solution Uptake

Fig. 6 exhibits the impedance modulus obtained at the lowest frequency (2 kHz) with resistive behavior ($\theta = 0^\circ$) for concrete samples in saturation tests made with CEM I and with different w/c ratio, $|Z|_{freq \rightarrow 0}$. The evolution of the values with immersion time corresponds to the expected results, with an initially sharp drop, followed by a decreasing evolution and a final stabilization. The more porous samples (higher w/c ratio) presented a severe impedance drop since the beginning of the saturation test and the lowest resistance values for longer immersion times. These results show that the values obtained for longer immersion times can be used to estimate the saturation time, t_s, and the apparent resistance, R_s. The dried concrete apparent resistance value, R_0, can be obtained by applying an extrapolation method to t = 0, i.e., for the beginning of the saturation test. The better linear relation is obtained representing admittance as function of the square root of immersion time.

Representation of the previous parameters for concrete samples in saturation tests made with CEM I and different w/c ratios show that the estimated dried apparent resistance, R_0, present relatively stable values (Fig. 7). This independency of the w/c ratio was expectable since this parameter should not be related with water content and ionic concentration. However, the saturation parameters are inversely dependent with w/c ratio, presenting higher saturation apparent resistance and time for lower w/c ratio, which is expected since this sample should have less porosity and solution uptake. The sample with a w/c ratio of 0.39 takes more time (7x) to be completely saturated comparatively to the sample with 0.6 w/c. Longer times needed for complete saturation can be due to the smallest pores and/or more important to the tortuosity, delaying the solution entrance. This trend suggests that further work must be developed to extract information from EIS results about the porosity parameters, like the porous dimension and/or their tortuosity. Fig. 8 depicts the results obtained from the permeability tests that were used as reference for this study. As can be observed, the

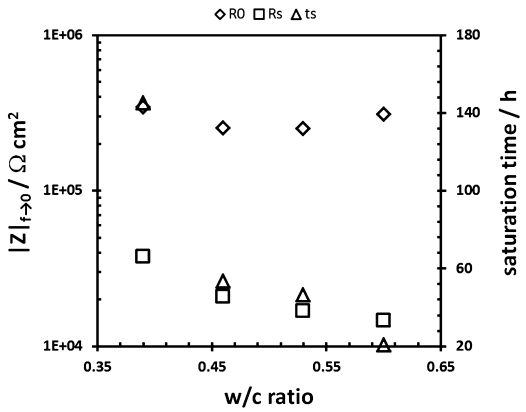

Fig. 7. Dried sample apparent resistance, extrapolated for t = 0, (R_0), saturation, apparent resistance (R_s) and saturation time (ts) correlation with w/c ratio obtained from, concrete samples with CEM I. These results were acquired from saturation tests and the, apparent resistance values were estimated from impedance modulus at the lowest, frequency (2 kHz) with resistive behavior ($\theta = 0^\circ$).

Table 3
Fitted parameters for concrete samples manufactured with a 0.5 w/c ratio and with different cement type, after 100 hours of drying (the units of R_1, R_2 and R_3 are in $\Omega\,cm^2$ while Y_0 units are $S\,s^n\,cm^{-2}$).

w/c = 0.5	Drying test (t = 100 h)										
	CPE1		R1	CPE2		R2	CPE3		R3	CPE4	
	Y_0	n		Y_0	n		Y_0	n		Y_0	n
CEM I	2.3E-12	1	1.9E+04	6.4E-11	0.85	2.4E+05	1.5E-07	0.49	4.0E+06	9.6E-09	0.79
CEM II/A	2.6E-12	1	5.7E+04	8.0E-11	0.84	2.1E+05	2.3E-07	0.50	8.7E+05	2.2E-07	0.57
CEM IV/A	2.3E-12	1	4.1E+04	1.2E-10	0.82	3.1E+05	1.0E-07	0.58	2.2E+06	7.6E-08	0.65

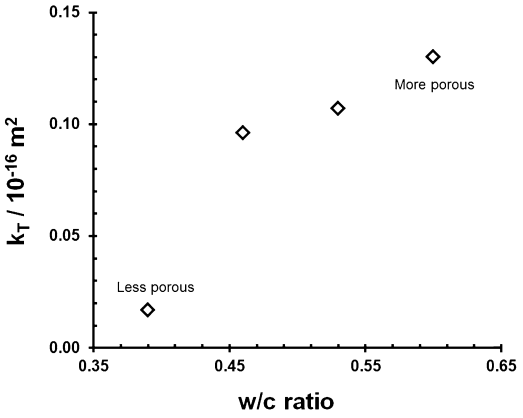

Fig. 8. Permeability results obtained for concrete samples with CEM I and for, different w/c ratio.

results follow the same trend which shows the coherency between both techniques, thus highlighting the fact that EIS is a powerful technique that can be used to assess the permeability of concrete samples.

Fig. 9 depicts the apparent resistivity behavior of concrete samples in saturation tests made with w/c = 0.39 and with different cement types. As stated before, the values of the apparent resistivity are approximately half of the real ones, considering the samples and cell geometry, the samples thickness and the total/exposed area ratio [43]. These apparent resistivity values were obtained, as previously, from impedance modulus at the lowest frequency (2 kHz) with resistive behavior ($\theta = 0^\circ$), considering an exposed area of 50 cm^3 and a sample thickness of 5 cm. At the beginning of the saturation test ($t \approx 0$), the resistivity values for the three types of concrete are quite different. The sample with CEM I revealed

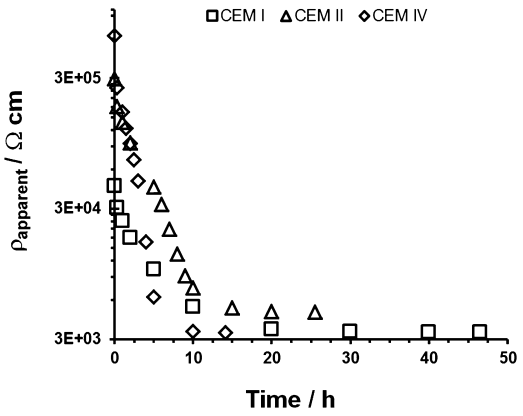

Fig. 9. E volution of the apparent resistivity with time for concrete samples in, saturation tests made with w/c≈0.53 (0.53 for CEM I; 0.51 for CEM II; 0.53 for, CEM IV) and with several cement type. The apparent resistivity was obtained from, impedance modulus at the lowest frequency (2 kHz) with resistive behavior ($\theta = 0^\circ$). An, exposed area of 50 cm3 and a sample thickness of 5 cm were considered.

the lowest value, while for the one with CEM IV the apparent resistivity is 14 times larger. The sample with CEM II has an intermediate value of 30 kΩ cm.

After 1 hour of immersion all the apparent resistivity values have decreased. The sample with CEM IV reveals the strongest reduction towards values that are 4 times smaller than the initial ones; while samples with CEM I showed a drop of approximately 1.8 times. After 2 hours of immersion the apparent resistivity values of samples with CEM IV showed a continuous decrease that was more marked comparatively to the other ones. At this stage the apparent resistivity values are equivalent to those obtained from samples with CEM II, and after 4 hours they become equal to the ones with CEM I. After 14 hours of immersion, the samples with CEM IV showed resistivity stabilization, revealing that full-saturation occurred, contrary to the other two samples in which the apparent resistivity values still retain a slow decrease. Finally, after 25.5 and 46.5 hours samples with CEM II and CEM I, respectively, stabilized in their lowest apparent resistivity values. It is also relevant to note that the values presented by the different samples are much closer than the initial apparent resistivity, in which samples with CEM I and CEM IV showed equivalent values around 3300 Ω cm, while the ones with CEM II showed a value of 4800 Ω cm.

3.3. *Diffusion Coefficients*

Traditionally, the EIS results can be used to estimate the water or solution uptake trend from several materials such as coatings. For that purpose the material must present a measurable dielectric behavior usually in the high frequency domain. However, for concrete samples, the response of the dielectric process on all measured system can only be slightly detected at very high frequencies. Consequently, solution uptake is difficult to determine as stated before, and it is extremely difficult to obtain the diffusion coefficients by traditional methods. However, since full immersed concrete samples (saturation tests) present a resistive behavior in almost all frequency regions, then the resistance can be easily estimated by the analysis of the EIS results. It is well-known that resistance is inversely dependent on the water content and concentration of ions. In the saturation tests very complex cross-processes occur with simultaneous solution and chloride ingress and ions leaching (OH^-, Ca^{2+}, etc.). Several authors showed that the main contributors to the ionic strength of the pore solution are the hydroxide and alkali ions and that conductivity of the pore solution can be estimated from these ions [44–46]. Thus, it seems a good approximation to accept that resistance is primarily related to solution uptake, ϕ, and that ionic strength solution inside concrete is nearly constant, then it is possible to assume $1/R \propto \phi$. Of course, there are other factors affecting the resistance such as porosity, tortuosity, etc., however, since concrete is a very heterogeneous material, then the resistance can be assumed as an average or statistical parameter, which correlates with pore parameters, presenting essentially average values. Thus, it is acceptable to assume that these parameters are not dependent upon the solution uptake. Assuming Fickian diffusion for transient-state and for short immersion times, then the parameters ϕ, ϕ_s, and ϕ_0 in equation 2

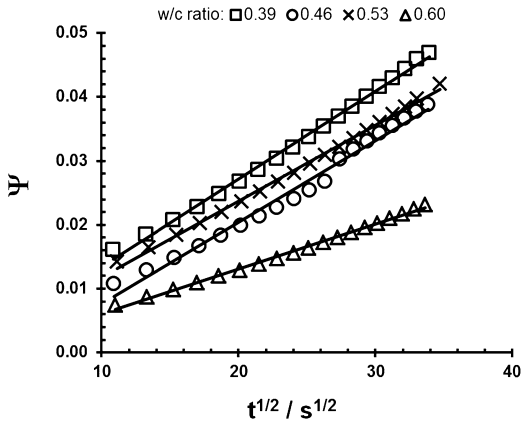

Fig. 10. Representation of the solution uptake function with the square root of the, time for concrete samples with CEM I and with different w/c ratio, obtained from, saturation tests.

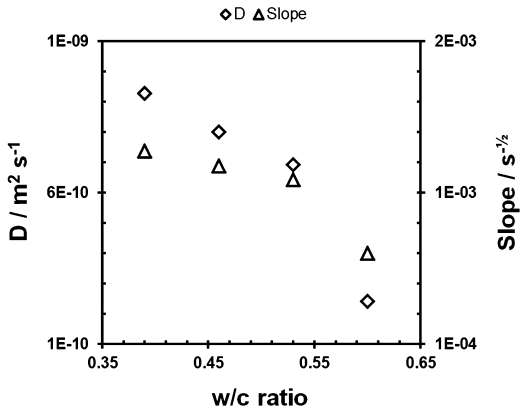

Fig. 11. Variation of diffusion coefficients (D) and curve slope with the w/c ratio, (concrete samples with CEM I). These results were obtained from saturation tests.

can be assessed using estimated resistances for a particular time t, R, for saturation time, R_s, and for dry condition by extrapolating the admittance to t = 0, R_0, respectively. These resistances can be obtained from saturation tests as showed previously, considering that the real resistivity values are approximately twice the values of the apparent ones [43]. Consequently, the following relation is a good approximation for diffusion processes occurring simultaneously at both faces:

$$\psi = \frac{1/R_0 - 1/R}{1/R_0 - 1/R_s} = \frac{4\sqrt{D}}{d\sqrt{\pi}}\sqrt{t} \quad (3)$$

in which D is the diffusion coefficient, t is the time, d is the samples thickness and ψ is the solution uptake function. It is worth of notice that ψ is obtained by a ratio of estimated admittances (inverse of resistance), assuming the considerations stated previously, then ψ can be only considered dependent from solution uptake.A linear relation between the solution uptake function, ψ, and the square root of time for the beginning of the saturation is obtained (fig. 10). Diffusion coefficient can be obtained by determining the slope of the curve and using the previous equation (fig. 11). The obtained diffusion coefficients values are in the range 2×10^{-10} and 1×10^{-9} m^2 s^{-1} which is the correct order of magnitude for this type of concrete. Despite that, an unexpected result occurred since the diffusion coefficient shows an inverse correlation with the w/c ratio. In normal conditions, higher w/c ratio leads to a greater amount of pores, as well an increasing in pores size. As reported previously, this fact leads to a permeability increase that should result in an increasing solution uptake kinetics and diffusion coefficient.

These misleading values can be explained observing fig. 12 in which the evolution of the solution uptake function values are presented as function of the square root of immersion time. The presented result is spanning from the beginning of the saturation test until complete saturation. In general, it is possible to divide the curves in three distinct regions:

(i) Short times, which corresponds to the part of the curve used to calculate the diffusion coefficient;
(ii) Intermediate times, where the value increases drastically;
(iii) longer times where there is a diminishing of the solution uptake function grow rate and a final stabilization.

In stage (i) samples with higher w/c ratio present lower values for the solution uptake function, ψ, which apparently indicates that the diffusion kinetic is more difficult to occur in more porous medium. However, initially the pores are filled with air that imposes difficulties for solution uptake. Since the tests were carried out at atmospheric pressure and because exchanges air/solution occurred along the same path, then for higher air content in the samples there is lower values for solution uptake function in that stage. Therefore, samples with higher w/c ratio must contain

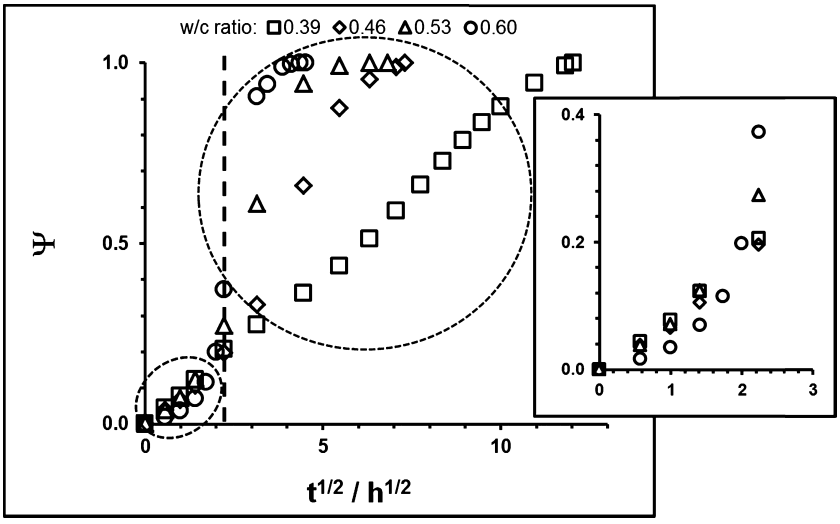

Fig. 12. Solution uptake function evolution with the square root of the time for, concrete samples with CEM I and with different w/c ratio, obtained from saturation, tests.

initially more air and should present lower diffusion coefficients. Thus, the diffusion coefficient obtained is not given by solution uptake, but is rather a complex parameter that initially is essentially related with the air diffusion, but latterly and progressively the solution diffusion has an increasing contribution.

The two following stages only appeared when air removal is almost complete and diffusion processes are essentially related with solution entrance. In stage (ii) the solution uptake function increased as normally observed in ordinary diffusion process and finally in phase (iii), the samples are near saturation and the process started to stabilize. The final results show that the relation between diffusion kinetics, diffusion coefficients and solution uptake are directly related with w/c ratio as expected.

The common methods to obtain equivalent data are based on removal of air from samples allowing the solution to fill the pores under vacuum to reach full saturation, as well as gravimetric methods for monitoring the saturation degree.

Probably the methodology used, at atmospheric pressure, is closer to the real situation found by concrete structures, and is undoubtedly more precise then the gravimetric methods.

4. Conclusions

The results of the EIS measurements, for immersed concrete samples, revealed that concrete can be considered a supported medium, except in the very high frequencies range. Thus, its contribution for the interpretation of the EIS results obtained from immersed reinforced steel concrete samples, only needs to take into account the bulk resistance.

For drying tests, concrete behaves as an unsupported medium and the interpretation of EIS results for steel reinforcing concrete samples must take into account the ionic charge separation. Two time constants appear in the EIS spectra, being related with ionic charge separation resulting from high and low mobility ions.

The diffusion coefficients obtained from EIS technique applied to concrete samples, for short immersion times, are strongly affected by the air content, i.e., by the porosity. The time necessary for air content release in concrete immersed samples can be assessed by EIS.

For longer immersion times the higher solution uptake kinetics and lower saturation time are directly related with higher w/c ratio and porosity.

Acknowledgement

The authors acknowledges FCT, Foundation for Science and Technology, for the financial support given to the project PTDC/ECM/105427/2008

References

[1] M. Hoseini, V. Bindiganavile, N. Banthia, Cement & Concrete Composites 31 (2009) 213–220.
[2] B. Feleko ÄŸlu, S. Turkel, B. Baradan, Building and Environment 42 (4) (2007) 1795–1802.
[3] A.M. Alshami, H.D.A. Imran, Cement and Concrete Research 32 (2002) 923–929.
[4] N. Neithalath, M. Sumanasooriya, O. Deo, Materials Characterization 61 (2010) 802–813.
[5] A. Królikowski, J. Kuziak, Electrochimica Acta 56 (23) (2011) 7845–7853.
[6] M.F. Montemor, A.M.P. Simões, M.M. Salta, Cement & Concrete Composites 22 (3) (2000) 175–185.
[7] C. Andrade, M. Keddam, X.R. Nóvoa, M.C. Pérez, C.M. Rangel, H. Takenouti, Electrochimica Acta 46 (2001) 3905–3912.
[8] M.A. Pech-Canul, P. Castro, Cement and Concrete Research 32 (3) (2002) 491–498.
[9] M. Ismail, M. Ohtsu, Construction and Building Materials 20 (2006) 458–469.
[10] J. Wei, X.X. Fu, J.H. Dong, W. Ke, Journal of Materials Science & Technology 28 (10) (2012) 905–912.
[11] J.R. Macdonald, D.R. Franceschetti, Journal of Electroanalytical Chemistry 99 (1979) 283–298.
[12] J.R. Macdonald, D.R. Franceschetti, Journal of Chemical Physics 68 (1978) 1614–1637.
[13] S. Gadve, A. Mukherjee, S.N. Malhotra, Construction and Building Materials 23 (1) (2009) 153–161.
[14] I.A. Wootton, L.K. Spainhour, N. Yazdani, Journal of Composites for Construction (2003) 339–347.
[15] X. Chen, S. Wu, Construction and Building Materials 38 (0) (2013) 804–812.
[16] V.C. Pereira, E.C. Monteiro, K. Almeida, Construction and Building Materials 40 (0) (2013) 710–718.
[17] S. Masoud, K. Soudki, Cement and Concrete Composites 28 (10) (2006) 969–977.
[18] N. Neithalath, J. Jain, Cement and Concrete Research 40 (7) (2010) 1041– 1051.
[19] X.R. Sánchez, X.R. Nóvoa, G. de Vera, M.A. Climent, Cement and Concrete Research 38 (7) (2008) 1015–1025.
[20] J. Crank, The Mathematics of Diffusion, 2ª Edition, Oxford University Press, 1979.
[21] F. Bellucci, L. Nicodemo, Corrosion 49 (1993) 235–247.
[22] R. Byron Bird, E. Warren, Stewart e Edwin N. Lightfoot, Transport Phenomena, 1st Edition, John Wiley & Sons, 1960.
[23] James R. Welty, Charles E. Wicks, Robert E. Wilson, Fundamentals of Momentum, Heat and Mass Transfer, 3ª Edition, John Wiley & Sons, 1984.
[24] A. da Costa, M. Fenaux, J. Fernández, E. Sánchez, A. Moragues, Construction and Building Materials 43 (2013) 217–224.
[25] L.-O. Nilsson, E., Poulsen, P., Sandberg, H.E. Sørensen, O., Klinghoffer, J.M. Frederiksen, Chloride Penetration into Concrete, State of the Art. Transport Processes, Corrosion Initiation, Test Methods and Prediction Models, HETEK Report No. 53, Road Directorate, 1996.
[26] A.T.C. Guimarães, M.A. Climent, G. de Vera, F.J. Vicente, F.T. Rodrigues a, C. Andrade, Construction and Building Materials 25 (2011) 785–790.
[27] V.B. Mišović-Stanković, D.M. Dražić, Z. Kačarević-Popović, Corrosion Science 38 (1996) 1513–1523.
[28] C. Perez, A. Collazo, M. Izquierdo, P. Marino, X.R. Nóvoa, Progress in Organic Coatings 36 (1999) 102–108.
[29] E.M. Rosen e, D.C. Silverman, Corrosion 46 (1990) 945–951.
[30] F. Bellucci, L. Nicodemo, Corrosion 49 (1993) 235–247.
[31] EN 197-1:2000 and NP EN 197-1:2001 (European and National Standard, respectively).
[32] R.D. Neves PhD Thesis in Civil Engineering, Instituto Superior Técnico (2012) [in Portuguese].
[33] R. Torrent, R., Materials and Structures 25 (6) (1992) 358–365.
[34] J.J. Kolleck, Materials and Structures 22 (3) (1989) 225–230.
[35] RILEM TC 116-PCD, Materials and Structures, 32 (3) (1999) 163–173.
[36] R. Dhir, P.C. Hewlett, Y.N. Chan, Magazine of Concrete Research 41 (148) (1989) 122–128.
[37] R. Torrent, G. Frenzer, Methoden zur messung und beurteilung der kennwerte des uberdeckungsbetons auf der baustelle - Teil 2, Switzerland (1995) [in German].
[38] B. Díaz, L. Freire, P. Merino, X.R. Nóvoa, M.C. Pérez, Electrochimica Acta 53 (2008) 7549–7555.
[39] C. Andrade, V.M. Blanco, A. Collazo, M. Keddam, X.R. Nóvoa, H. Takenouti, Electrochimica Acta 44 (1999) 4313–4318.
[40] M. Cabeza, M. Keddam, X.R. Nóvoa, 1, I. Sánchez, H. Takenouti, Electrochimica Acta 51 (2006) 1831–1841.
[41] M. Cabeza, P. Merino, A. Miranda, X.R. Nóvoa, I. Sanchez, Cement and Concrete Research 32 (2002) 881–891.
[42] C. Andrade, C. Alonso, X.R. Nóvoa, M. Keddam, H. Takenouti, Cement and Concrete Research 27 (8) (1997) 1191–1201.
[43] B. Díaz, L. Freire, X.R. Nóvoa, B. Puga, V. Vivier, Cement and Concrete Research 40 (2010) 1465–1470.
[44] B. Lothenbach, F. Winnefeld, Cement and Concrete Research 36 (2) (2006) 209–226.
[45] K.A. Snyder, X. Feng, B.D. Keen, T.O. Mason, Cement and Concrete Research 33 (6) (2003) 793–798.
[46] Nilla Olsson, Véronique Baroghel-Bouny, Lars-Olof Nilsson, Mickaël Thiery, Cement & Concrete Composites 40 (2013) 40–47.